RAIO-0819-66530

August 02, 2019

Docket No. 52-048

U.S. Nuclear Regulatory Commission
ATTN: Document Control Desk
One White Flint North
11555 Rockville Pike
Rockville, MD 20852-2738

SUBJECT: NuScale Power, LLC Supplemental Response to NRC Request for Additional Information No. 202 (eRAI No. 8911) on the NuScale Design Certification Application

REFERENCES:

1. U.S. Nuclear Regulatory Commission, "Request for Additional Information No. 202 (eRAI No. 8911)," dated August 25, 2017
2. NuScale Power, LLC Response to NRC "Request for Additional Information No. 202 (eRAI No.8911)," dated December 21, 2018
3. NuScale Power, LLC Supplemental Response to NRC "Request for Additional Information No. 202 (eRAI No. 8911)," dated April 9, 2019
4. NuScale Power, LLC Supplemental Response to NRC "Request for Additional Information No. 202 (eRAI No. 8911)," dated May 1, 2019
5. NuScale Power, LLC Supplemental Response to NRC "Request for Additional Information No. 202 (eRAI No. 8911)," dated June 3, 2019

The purpose of this letter is to provide the NuScale Power, LLC (NuScale) supplemental response to the referenced NRC Request for Additional Information (RAI).

The Enclosures to this letter contain NuScale's supplemental response to the following RAI Question from NRC eRAI No. 8911:

- 03.09.02-18

Enclosure 1 is the proprietary version of the NuScale Supplemental Response to NRC RAI No. 202 (eRAI No. 8911). NuScale requests that the proprietary version be withheld from public disclosure in accordance with the requirements of 10 CFR § 2.390. The enclosed affidavit (Enclosure 3) supports this request. Enclosure 2 is the nonproprietary version of the NuScale response.

This letter and the enclosed responses make no new regulatory commitments and no revisions to any existing regulatory commitments.

If you have any questions on this response, please contact Marty Bryan at 541-452-7172 or at mbryan@nuscalepower.com.

Sincerely,

Thomas A. Bergman
Vice President, Regulatory Affairs
NuScale Power, LLC

Distribution: Gregory Cranston, NRC, OWFN-8H12
Samuel Lee, NRC, OWFN-8H12
Marieliz Vera, NRC, OWFN-8H12

Enclosure 1: NuScale Supplemental Response to NRC Request for Additional Information eRAI No. 8911, proprietary

Enclosure 2: NuScale Supplemental Response to NRC Request for Additional Information eRAI No. 8911, nonproprietary

Enclosure 3: Affidavit of Thomas A. Bergman, AF-0819-66531

Enclosure 1:

NuScale Supplemental Response to NRC Request for Additional Information eRAI No. 8911, proprietary

Enclosure 2:

NuScale Supplemental Response to NRC Request for Additional Information eRAI No. 8911, nonproprietary

NuScale Power, LLC
1100 NE Circle Blvd., Suite 200 Corvalis, Oregon 97330, Office: 541.360.0500, Fax: 541.207.3928
www.nuscalepower.com

Response to Request for Additional Information
Docket No. 52-048

eRAI No.: 8911
Date of RAI Issue: 08/25/2017

NRC Question No.: 03.09.02-18

10 CFR 52.47 requires the design certification applicant to include a description and analysis of the structures, systems, and components (SSCs) sufficient to permit understanding of the system designs. TR-0916-51502-P, Rev. 0, “NuScale Power Module Seismic Analysis” describes the methodologies and structural models that are used to analyze the dynamic structural response due to seismic loads acting on the NuScale Power Module (NPM). The description is insufficient for staff to reach a safety finding. Specifically, the report does not provide the seismic and LOCA stress results. Please provide the seismic analysis details and stress results under Service Level D condition for the following reactor internals components. Include the requested information in the NPM Seismic Report or in separate reports.

- core support assembly (core barrel, lower core plate, reflector, upper core plate, upper core support)
- lower riser assembly
- upper riser assembly (upper riser, upper riser hanger support)
- control rod assembly guide tube, control rod assembly guide tube support, control rod assembly card, control rod drive shaft, and control rod drive shaft support
- steam generator tubes and tube supports
- control rod assembly guide tubes

The component analysis should include a brief description of the component structure modelling, input motion (time history or in-structure response spectrum), major assumptions, acceptance criteria under Service Level D condition including stress and deflection limits, fluid modelling, mass distribution, damping values, gap considerations, dominant modes and frequencies, and seismic and LOCA stress results and ASME B&PV Code Section III stress evaluation under Service Level D condition.

NuScale Response:

The initial response to RAI 8911 Question 03.09.02-18 was submitted by NuScale in letter RAIO-1218-63980, dated December 21, 2018. Supplements to the initial response were submitted by NuScale in letter RAIO-0419-65152, dated April 9, 2019 (03.09.02-18S1), RAIO-0419-65386, dated May 1, 2019 (03.09.02-18S2), and in letter RAIO-0619-65808, dated June 3, 2019 (03.09.02-18S3). This response responds to the remaining NRC open questions regarding the RVI and SG service level D stress analyses. Additionally, this response revises the stress results included in previous responses with updated results based on revised seismic and DBPB (i.e., blowdown) loads where applicable.

Open Question RVI 1 - The response to RAI 8911 03.09.02-18S3 was submitted to provide justification for not explicitly considering the diametric gaps between the CRDS and CRAGT and their associated supports in the stress analysis of those components. During a follow-up call on July 3, 2019, the NRC requested justification for why the seismic input that was used for 03.09.02-18S3 was limiting. NuScale agreed to provide this justification and, given that the seismic analysis had been revised, either confirm that the case "S7CS_CAP_CR_RXM1_NomiK" remains the limiting case in terms of applicable locations and dominant frequencies, or identify the new case used.

NuScale Response - The justification for modeling the CRDS gap as linear has been updated to use the current seismic inputs and to include an evaluation of all twelve seismic cases (rather than a single limiting one). The revised justification is included as Attachment C and supersedes the information provided in RAI 8911 03.09.02-18S3 in its entirety.

Open Question RVI 12 - In RAI 8911 03.09.02-18S3, NuScale agreed to provide stress analysis results for the core support block assembly including the hex head cap screw, shear pin, welds, top plate and gusset plate.

NuScale Response - The stress analysis of the core support block assembly has been completed and the results are included in Attachment A. For the stress results for the hex head cap screw, alignment dowel, core support block top plate and core support block gusset see Table A-10. The welds between the core support block gussets and the RPV bottom head are within the jurisdictional boundary of the RPV and classified as NB per NB-1132.2(d), and therefore, are outside the scope of this analysis.

Open Question RVI 18 - In RAI 8911 03.09.02-18S2, NuScale agreed to provide finalized stress ratios with updated seismic loads when available.

NuScale Response - The stress analysis of the reactor vessel internals using the revised seismic loads has been completed. Attachment A includes an updated description of the evaluation and summary of stress results that supersedes the information provided in the response to RAI 8911 Question 03.09.02-18S2.

Open Question SG 5 - In 03.09.02-18S1 NuScale agreed to either provide stress results for the SG components that include the MSPB and FWPB loads or to justify that MSPB and FWPB loads are bounded by the LOCA loads.

NuScale Response - MSLB and FWLB loads have been calculated and are bounded by LOCA loads. Therefore, they are not included in the Level D SG stress analysis. This evaluation is discussed further in Attachment B.

Open Question SG 9 - During phone call with the NRC on February 6, 2019, NuScale agreed to provide updated stress analysis results for the SG components and supports using the revised seismic loads.

NuScale Response - The stress analysis of the steam generator and supports using the revised seismic loads has been completed and the results are included in Attachment B in Tables B-7 through B-12.

Attachment A - Reactor Vessel Internals (RVI)

General Information

Detailed stress analysis for the reactor vessel internals (RVI) under Service Level D conditions was performed in accordance with the American Society for Mechanical Engineers (ASME) Boiler and Pressure Vessel Code (BPVC). Analysis details and stress results are summarized below.

The components and welds included in this evaluation are listed in Table A-1 and Table A-2 below.

Depending on whether seismic and loss of coolant accident (LOCA) forces and moments are available for a component under analysis, one of two major methodologies is used in this calculation. In the category “1” methodology, forces and moments are applied at the bounding cross section of the components and associated welds. For components with simple geometries, primary stresses are calculated using closed form equations. In the case of more complicated geometry, forces and moments are applied to a finite element (FE) model of the component and stresses are derived using a static FE analysis. The category “2” methodology is used when seismic and LOCA forces and moments are not available. In this case, response spectra are defined at the item supports and stresses are derived from the FE analysis. The applicable methodology for each component and weld included in this analysis is provided in Table A-1 and Table A-2.

Assumptions

1. Bellows concentric plate dimensions: The dimensions of the URVI bellows concentric plates are not yet finalized as the component details are to be provided by the supplier. The analysis performed on this component is based on a computer aided design (CAD) model.

Input loading

The load combinations applicable to this analysis are provided in Table A-3. Each of the loads provided in Table A-3 is discussed, below.

1. Operating pressure difference (PD): The operating pressure difference across the internals does not vary significantly for different power levels. Therefore, this load is not included in the analysis.
2. Deadweight (DW): For the category “1” methodology, DW is applied as reaction forces and moments. For the category “2” methodology, DW is added as a separate loadstep in the analysis.
3. Buoyancy (B): The reaction forces and moments (category “1” methodology) used for DW include buoyancy effects. For the category “2” methodology, buoyancy is not included and therefore the full DW is considered. This provides minimal conservatism as the full DW contributes a small amount of stress to the final stress as compared to other applicable Level D loads.
4. Mechanical Loads such as RVI support reactions, fuel assembly weight, SCRAM Loads (EXT): A mechanical SCRAM load of {{ }}[2(a)(c)] per CRA is included in the analysis where applicable. Note that fuel assembly weight is included in the DW loading. RVI support reactions are captured in DW, LOCA, and SSE loads.
5. Rod ejection accident (REA): REA is not applicable.
6. Main steam pipe break/feedwater pipe break/design basis pipe break (MSPB/FWPB/LOCA): MSPB and FWPB loads are not applicable to the components analyzed in this evaluation. LOCA loads (i.e. design basis loss of coolant accident (LOCA) loads) are applied as reaction forces and moments or as accelerations in static analysis.
7. SSE (Safe Shutdown Earthquake): Reaction forces and moments, ISRS, or time histories are used. A constant composite structural damping ratio of 4% is used for the multi-point response spectrum analysis.
8. Based on the loading information provided above, the loads applicable to the lower core plate (LCP) analysis are DW + SCRAM ± SRSS (SSE + LOCA). For other components, the required loads are DW ± SRSS (SSE + LOCA).

Component structural modeling

Modeling details are provided below for components analyzed via FE analysis.

1. Upper core plate (UCP)

   Figure A-1 shows the model of the UCP. The element types are provided in Table A-5. Note the model was created based on a previous configuration of the bolt holes rather than the configuration currently documented in the NuScale Power Module (NPM) design drawings. This is acceptable because the boundary conditions are applied at the

circumference of the UCP and no loads are applied on the bolt holes, so the bolt hole configuration has no effect on the analysis of the plate. (The stress evaluation of the UCP tabs is performed using the current configuration of the tab and closed form equations.)

A static analysis is performed for the UCP. The applicable loads are the DW, SSE, and LOCA forces and moments (category "1" methodology) provided at the lower riser-UCP interface {{ }}[2(a)(c)]. The combined loads are applied to a single pilot node at the center of the UCP. This pilot node is connected to 36 slave nodes, as shown in Figure A-1, where each slave node is created at the fuel assembly location. Each slave node is tied to each of the fuel pin holes using contact pairs. Therefore, the load is transferred from the pilot node to the slave nodes and then to the pin holes. This distributes the load across the entire plate for a realistic distribution of forces.

The boundary conditions are applied at the circumference of the UCP. Here, all six degrees of freedom (DOF) are constrained as shown in Figure A-1.

2. Lower core plate (LCP)

Figure A-2 shows the model of the LCP. The element types are provided in Table A-5. Some of the holes in the LCP are shifted or excluded from the FE model. The effect of these shifts or exclusions is negligible because the highest stresses in the LCP are in the grids (fuel assembly locations) and not near these holes. Therefore, using this FE model for stress analysis is acceptable.

A static analysis is performed for the LCP. The applicable loads are the SCRAM vertical force and the DW, SSE, and LOCA forces and moments (category "1" methodology) provided at the reflector-LCP-core barrel interface {{ }}[2(a)(c)]. The combined loads are applied to a single pilot node at the center of the LCP. This pilot node was connected to 36 slave nodes, as shown in Figure A-2, where each slave node is created at the fuel assembly location. Each slave node is tied to each of the fuel pin holes using contact pairs. Therefore, the load is transferred from the pilot node to the slave nodes and then to the pin holes. This distributes the load across the entire plate for a realistic distribution of forces.

The boundary conditions are applied at the circumference of the LCP. Here, the six DOFs are constrained as shown in Figure A-2.

3. Upper riser hanger ring

   Figure A-3 shows the model of the upper riser hanger ring. The element types are provided in Table A-6. This model was created based on a previous configuration of the hanger ring rather than the configuration currently documented in the NPM design drawings. However, since the previous configuration has less total material and since the holes are larger in this configuration, the stresses and deformation calculated from the previous configuration are larger and thus more conservative. On the other hand, the new configuration adds approximately 650 lbm. This added mass has negligible effect on the upper riser hanger ring stress as compared to the other applicable loads. Therefore, it is acceptable to use the previous configuration for analysis.

   A static analysis is performed for the upper riser hanger ring. The applicable loads are the DW, LOCA, and SSE forces and moments (category “1” methodology) provided at each hanger brace. The combined loads are applied at the hanger brace attachment points in the local coordinate systems for the braces.

   The ring is constrained in the Y translation DOF at the 8 bolt holes which attach the hanger ring to the baffle plate. The horizontal translational DOFs at these locations are not constrained because the horizontal loads are not carried by these threaded fasteners. Instead, the horizontal constraints are applied to a side surface of the ring to represent the confinement below the Upper Riser Hanger Braces. This is shown in Figure A-3.

4. Control rod assembly (CRA) guide tube assembly
   a. Overview

      The CRA guide tube assembly is composed of four components: CRA guide tube, CRA cards, CRD shaft alignment cone, and CRA lower flange. There are no available loads in form of forces and moments for the CRA guide tube assembly. Loads acting on the assembly are generated by performing a response spectra analysis for SSE loads and a static analysis of LOCA accelerations (category “2” methodology). Prior to the SSE response spectrum analysis, a modal analysis is performed. The modal analysis is run for 100 modes to capture the dynamic effect due to seismic events.

      Considering the control rod assembly in a variety of parking positions (see Fluid modeling and mass distribution information, below), three ANSYS analyses are

performed.

Figure A-4 shows the basic geometry and mesh of the CRA guide tube assembly model. The element types are provided in Table A-7.

Figure A-5 shows pilot nodes at which the response spectra are applied. This figure also shows the simulated constraints with the guide tube support plate (GTSP) and the UCP. These constraints are realized through multi-point constraint (MPC), as shown in Figure A-6. CRA cards, the alignment cone, and the lower flange are also attached to the tube via bonded contact elements as shown in the same figure.

b. Fluid modeling and mass distribution

To account for added mass of water inside the CRA guide tube assembly, the mass density of the CRA tube is adjusted by adding the mass of water contained inside the CRA guide tube assembly.

Interaction (“parking”) of the control rod is also accounted for. The control rod may be in a variety of positions - from rod completely inserted into fuel to fully elevated. In case of fully inserted control rods, only the alignment cone supports part of the CRD shaft. In the case of the control rods in the fully elevated position, the entire CRA guide tube assembly provides support for the CRD shaft.

The interaction of the control rods is simulated using mass elements. For conservatism, the entire mass of the control rods is imposed on the alignment cone for the case of the rod completely elevated. Similarly, for the cases where the rod is partially elevated, the entire mass of the control rod is distributed to two of the longest “fingers” of the top card and then, in a separate run, the entire mass of the control rod is distributed to the second card from top of the CRA guide tube. The added mass locations for these three cases are illustrated in Figure A-7.

5. CRA guide tube support plate (GTSP)

The CRA GTSP supports the top of the CRA. Static analysis is performed on the CRA GTSP. Loads acting on the CRA GTSP are extracted from the CRA analysis documented above (category “1” methodology). There are 16 CRAs supported by the CRA GTSP. The 16 locations are loaded through pilot nodes that distribute loads into the interface of the plate with the CRAs. Figure A-8 shows the CRA GTSP model and

boundary conditions. The element types are provided in Table A-5.

Connection of the CRA GTSP to the lower riser spacer is not modeled. Nodes at the CRA GTSP-spacer interface are instead constrained in all degrees of freedom. This simplification has negligible impact on stresses and is therefore acceptable.

6. Upper riser assembly

   a. Overview

      The Upper Riser Assembly (URA) is composed of upper CRD shaft supports, upper riser transition, upper riser section, upper riser hanger ring, upper riser hanger braces, and upper riser bellows. The 16 CRD shafts are also included in the structural model. The entire URA is made of type 304/304L stainless steel material, except for the CRD shafts which use type 410 stainless steel. There are no available loads in form of forces and moments for the URA. Loads acting on the URA are generated by performing a response spectra analysis for SSE loads and static analyses of LOCA accelerations (category “2” methodology). Prior to the SSE response spectrum analysis, the modal analysis was run for 2000 modes in order to capture an effective mass of at least 80 percent.

      Figure A-9 depicts the basic geometry and mesh of the URA model. The element types used in the model are listed in Table A-4. The contacts are bonded except for the bellows lateral restraints as shown in Figure A-10. Constraints of the model are illustrated in Figure A-11. The FE meshes for the CRD shaft and CRD shaft supports are shown in Figure A-12 and Figure A-13, respectively.

   b. Fluid modeling and mass distribution

      To account for added mass of water inside the URA, the mass density of the URA is adjusted by adding the mass of water contained inside the URA assembly. A similar approach is taken for the drive shafts; the total mass is evenly distributed in PIPE288 elements. MASS21 elements are added to the ends of the drive shafts to account for the mass of the control rod assemblies.

Acceptance criteria

Per paragraph NG-3225 of Section III, Subsection NG, the rules of ASME BPVC Appendix F are to be used for Level D conditions. In addition, when the special stress limits of NG-3227 are applicable for Level D Limits, the calculated stresses shall not exceed twice the stress limits given in NG-3227 as applied for Level A and Level B Service Limits.

The applicable qualification criteria from ASME BPVC Table F-1200-1 and paragraph NG-3227 are summarized as follows:

1. F-1331.1 for general primary membrane stresses, local primary membrane stresses, general or local membrane plus bending primary stresses for components.
2. NG-3227.1(a) for bearing stress for components. Note that F-1331.3 is bounded by NG-3227.1(a).
3. F-1331.1(d) and NG-3227.2(a) for average primary pure shear stress of components.
4. F-1334.3 and F-1334.5 for buckling of components.
5. F-1331.1(a) for allowable tensile stress of threaded structural fasteners.
6. F-1331.1(d) for allowable shear stress of threaded structural fasteners.

The fasteners evaluated in this calculation are the Upper Alignment Hanger Threaded Structural Fastener, the Hex Head Cap Screw, and Socket Head Cap Screw. These are classified as Internal Structure and Core Support Structure, respectively, in the NPM design drawings. Per the Design Specification, the Internal Structure is designed using NG-3000, which defines the criteria for Core Support Structures. Therefore, the fasteners in this calculation are qualified using the rules for Core Support Structures. Classification of these parts as threaded structural fasteners, as opposed to bolts, is justified as these parts do not form part of the pressure retaining boundary (see ASME BPVC, subparagraph NG-3231(b)).

Since the ultimate strength of these threaded structural fasteners is less than 100 ksi, per ASME BPVC F-1440(d), the requirements F-1331.4, and therefore the rules of F-1335, are not applicable. Additionally, the special stress limits defined in NG-3227 are not applicable to threaded structural fasteners. Thus, the stress limits for the threaded structural fasteners analyzed in this calculation are determined in accordance with F-1331.1. Specifically, general primary membrane stress intensity is evaluated in accordance with F-1331.1(a) and the average primary shear stress across a section loaded in pure shear is evaluated in accordance with F-1331.1(d).

The Pm+Pb criteria in F-1331.1(c) is not needed because the bending moments on these fasteners are insignificant due to their arrangement.

Table A-8 summarizes the applicable stress limits.

The qualification criterion for welds is provided in ASME BPVC paragraph NG-3352 and is noted below:

> *The quality factor is used by multiplying the allowable stress limit for primary and secondary categories times the quality factor in evaluating the design. The use of weld quality factor n is for static, not fatigue applications.*

Therefore, the allowable stresses for welds are the stress limits in Table A-8 multiplied by a quality factor n, where n is provided in ASME BPVC Table NG-3352-1. Table A-9 summarizes weld types and their applicable quality factors.

Relative displacements between adjacent the control rod drive (CRD) shaft grids are evaluated. Note that there are no specific limits for the displacements and results are provided for information only.

Results

1. Modal results

    a. CRA guide tube assembly

    The modal results from CRA_1 analysis are shown in Figure A-14, indicating the major horizontal modes are at {{ }}$^{2(a)(c)}$ Hz and major vertical mode at {{ }}$^{2(a)(c)}$ Hz. Figure A-15 shows the modal shape of the first horizontal major mode. The results for CRA_2 and CRA_3 are in a similar trend except that the major horizontal modes for CRA_2 and CRA_3 are {{ }}$^{2(a)(c)}$ Hz and {{ }}$^{2(a)(c)}$ Hz, respectively.

    b. Upper riser assembly

    The modal results are shown in Figure A-16 and Figure A-17, indicating the major horizontal mode at {{ }}$^{2(a)(c)}$ Hz and major vertical mode at {{ }}$^{2(a)(c)}$ Hz. The first four dominant frequencies and mode shapes for the CRD shaft are shown in Figure A-18. Note that while only one shaft is illustrated, all 16 shafts

behave the same.

2. Stress results

   Stress results are compared to ASME BPVC requirements in Table A-10 and Table A-12 for components and welds, respectively. The locations where the stress ratio are greater than 0.8 are summarized in Table A-11 and Table A-13 for components and welds, respectively.

   Whether or not path lines are used is dependent upon the stress results. If the maximum total stress intensity for a component is less than the Pm, the maximum total stress intensity is conservatively used for both Pm and (Pm+Pb) qualifications. Otherwise, path lines are assigned to calculate and print linearized stresses.

   Path lines were assigned in LCP, upper riser hanger ring, and the CRA GTSP. For the LCP model, the resulting stress intensity for the analysis is shown in Figure A-19. Four path lines, shown in Figure A-20, were created near the maximum stress intensity location. The path lines #1 and #2 are through the thickness of the plate, while the path lines #3 and #4 are through the radial ligament of the holes. For the upper riser hanger ring model, the resulting stress intensity for the analysis is shown in Figure A-21. A total of 16 path lines (two for each hole), shown in Figure A-22, are created near the highest stress locations. For the CRA GTSP model, the stress classification lines shown in Figure A-23 represent the through thickness locations in a single quadrant. These same positions are repeated in each quadrant.

3. Deflections

   Maximum relative displacements between adjacent CRD shaft grids are provided in Table A-14. Since the maximum value ({{ }}$^{2(a),(c)}$) is insignificant, it is concluded that the CRD shafts do not experience excessive displacements.

Conclusions

The analysis described above demonstrates that the design of the RVI satisfies the structural requirements of the ASME BPVC for Service Level D loads.

Table A-1. Components

Item	Part Number	Methodology
Upper Riser Transition	A023.300	1
Upper Riser Section	A023.301	2
Upper CRD Shaft Support	A023.305	2
Top CRD Shaft Support(1)	A023.312	2
Upper Riser Hanger Ring	A023.306	1
Upper Riser Hanger Brace	A023.307	1
Upper Alignment Hanger Threaded Structural Fastener	A023.309	1
Upper Riser Bellows	A023.310	2
Upper Core Plate (UCP)	A023.200	1
Lower Riser Section	A023.201	1
Lower Riser Transition	A023.202	1
Lower Riser Spacer	A023.203	1
In-core Instrument Guide Tube (ICIGT) Support	A023.210	2
CRA Guide Tube Support Plate (GTSP)	A023.230	1
CRA Guide Tube	A023.231	2
CRD Shaft Alignment Cone	A023.232	2
CRA Card	A023.233	2
CRA Lower Flange	A023.234	2
Fuel Pin Cap	A023.250	1
Fuel Pin	A023.251	1
	A023.061	1
Core Barrel	A023.009	1
Reflector Block	A023.044-046	1
Upper Support Block	A023.047-048	1
Reflector Block Alignment Pin	A023.049	1
Lower Core Plate (LCP)	A023.008	1
Socket Head Cap Screw(2)	A011.043	1
Control Rod Drive Shaft	01D4484H01, 01D4485H01, 01D4486H01, (Drive Shaft Sections)	2
Hex Head Cap Screw 1.25-12UN-4.5IN	A010.075	1
Core Support Block Gusset	A011.040-041	1
Core Support Block Top Plate	A011.042	1
Alignment Dowel	A011.045	1

Notes:

1. The Top CRD shaft Support (A023.312) is structurally equivalent to the Upper CRD shaft Support (A023.305). For the remainder of the document, use of the term “Upper CRD shaft Support” covers both components.
2. A011.043 is also referred to as a “Hex Head Cap Screw” in the NPM design drawings. The term “Socket Head Cap Screw” is used to describe all instances of part A011.043 for the remainder of this document.

Table A-2. Welds

Weld Number	Description	Methodology
A023.300.001	Upper Riser Transition Seam	1
A023.301.001	Upper Riser Section Seam	1
A023.305A-D.001 -A023.305A-D.008, A023.312.001-008	Upper CRD Shaft Support	2
A023.307A-H.001	Brace to Upper Riser Hanger Ring	1
A023.307A-H.002	Brace to Upper Riser Section	1
A023.310.001	Upper Riser to Bellows	1
A023.310.002	Bellows to Upper Riser Transition	1
A023.200.001	Lower Riser to UCP	1
A023.201.001	Lower Riser Section	1
A023.202.001	Lower Riser Transition	1
A023.203.001	Lower Riser Spacer	1
A023.203.001A	Lower Riser Spacer to Lower Riser Section	1
A023.203.002	Lower Riser Transition to Lower Riser Spacer	1
A023.210.001A-H	ICIGT Support to Lower Riser Transition	1
A023.230.001A-D	CRA GTSP to Lower Riser Spacer	1
A023.231.001A-P	CRA Lower Flange to CRA Guide Tube	2
A023.231.002A-P -A023.231.009A-P	CRA Card to CRA Guide Tube	2
A023.231.010A-P -A023.231.013A-P	CRDS Alignment Cone	2
A023.009.001 -A023.009.004	Upper Support Block	1
A023.008.001	Core Barrel to LCP	1

Table A-3. Required load combinations

Plant Event	Service Level	Load Combination	Allowable Limit
Rod Ejection Accident	D	PD + DW + B + EXT + REA	Level C
Main Steam and Feedwater Pipe Breaks	D	PD + DW + B + EXT + MSPB-FWPB	Level D
SSE + DBPB-MSPB-FWPB	D	PD + DW + B + EXT ± SRSS (SSE + LOCA-MSPB-FWPB)	Level D

Note: SRSS is the square root sum of the squares

Table A-4. Element types in URA model

Item	Element Type
Control Rod Drive Shaft	PIPE288
URVI Section	SHELL181
Control Rod mass	MASS21
Contact pairs	TARGE170, CONTA174, CONTA175
Other components	SOLID45

Table A-5. Element types in UCP, LCP, and CRA Guide Tube Support Plate models

Item	Element Type
Section	SOLID45
Contact pairs (for scoped pilot node to apply loads)	TARGE170, CONTA174

Table A-6. Element types in upper riser hanger ring model (ANSYS Workbench)

Item	Element Type
Section	SOLID187,SOLID186
Contact pairs (for scoped pilot node to apply moment loads)	TARGE170, CONTA174
Non-structural surface to apply pressure (converted from force loads)	SURF154

Table A-7. Element types in CRA Guide Tube Assembly model

Item	Element Type
CRA Guide Tube (teal in Figure A-4)	SHELL181
Other components (purple in Figure A-4)	SOLID45
Contact pairs (for scoped pilot node to apply loads and to bond Shell and Solid elements)	TARGE170, CONTA174, CONTA175
Control Rod mass	MASS21

Table A-8. Allowable stress limits for Level D

	Stress Category	Code Paragraph	Criterion
Component	General primary membrane stress, Pm	F-1331.1(a)	lesser of 2.4Sm and 0.7S_u
	Local primary membrane stress, Pl	F-1331.1(b)	1.5Pm
	General or local primary membrane plus bending stress, Pm+Pb	F-1331.1(c)(1)	1.5Pm
	Bearing stress	NG-3227.1(a)	2Sy(1)
	Average primary pure shear stress	F-1331.1(d), NG-3227.2(a)	lesser of 0.42Su and 1.2Sm
	Compressive loads	F-1334.3,F-1334.5	Multiple criteria
Threaded Structural Fastener(2)	Tensile stress	F-1331.1(a)	lesser of 2.4Sm and 0.7S_u
	Shear stress	F-1331.1(d)	0.42S_u

Notes:

1. This is for general bearing stress, which bounds the 2.1Su (F-1336 for pinned joints) and 3Sy (NG-3227.1(a) for bearing stress distance to free edge distance larger than distance over which the bearing load is applied). Therefore, the 2Sy limit is conservatively used in this document.
2. See the *'Acceptance criteria'* section, 3rd through 5th paragraphs.

Table A-9. Weld geometry summary

Component 1	Component 2	Weld Geometry and Size	Weld Category and Type	Quality Factor n(1)
Upper Riser Hanger Brace (A023.307)	Upper Riser Hanger Ring (A023.306)	{{		
Upper Riser Hanger Brace (A023.307)	Upper Riser Section (A023.301)			
Upper CRDS Support (A023.305)	Upper Riser Section (A023.301)			
Upper Riser Bellows (A023.310)	Upper Riser Transition (A023.300)			
ICIGT Support (A023.210)	Lower Riser Transition (A023.202)			
Lower Riser Spacer (A023.203)	Lower Riser Section (A023.201)			
Lower Riser Section (A023.201)	Upper Core Plate (A023.200)			
CRA GTSP (A023.230)	Lower Riser Spacer (A023.203)			
CRA Guide Tube (A023.231)	CRA Alignment Cone (A023.232)			
CRA Card (A023.233)	CRA Guide Tube (A023.231)			
CRA Lower Flange (A023.234)	CRA Guide Tube (A023.231)			
Upper Support Block (A023.048)	Core Barrel (A023.009)			}}2(a)(c)
Core Barrel (A023.009)	Lower Core Plate (A023.008)	{{		
Upper Riser Section (A023.301)	Upper Riser Bellows (A023.310)			
Lower Riser Transition (A023.202)	Lower Riser Spacer (A023.203)			}}2(a)(c)

Notes:

1. Assuming using surface visual examination method except note (2).
2. Assuming using root and final PT or MT examination method based on the geometry
3. Assuming using RT or UT and PT or MT examination method based on the geometry

Table A-10. ASME BPVC compliance - components

Item (Part Number)	Stress Type	Stress Ratio
Upper Riser Transition (A023.300)	Pm	{{
	Pm+Pb	
	τ	
Upper Riser Section (A023.301)	Pm	
	Pm+Pb	
Upper CRDS Support (A023.305)	Pm	
	Pm+Pb	
Upper Riser Hanger Ring (A023.306)	Pm	
	Pm+Pb	
Upper Riser Hanger Brace (A023.307)	Pm	
	Pm+Pb	
	τ	
Upper Alignment Hanger Threaded Structural Fastener (A023.309)	Tensile stress in stud, σns	
	σbearing	
	Shear stress in stud threads, τs	
	Shear stress in hanger ring threads, τn	
Upper Riser Bellows (A023.310)	Pm	
	Pm+Pb	
Upper Core Plate (A023.200)	Pm	
	Pm+Pb	
	τ	
	σbearing	
	Pm	
	Pm+Pb	
Lower Riser Section (A023.201)	Pm	
	Pm+Pb	
	τ	
	Compressive stress, σbu_c	
	Combined axial compression and bending, NF-3322.1(e)(1), eq. 20,σbu_cs_20	
	Combined axial compression and bending, NF-3322.1(e)(1), eq. 21, σbu_cs_21	
	Combined axial compression and bending, NF-3322.1(e)(1), eq. 22, σbu_cs_22	
Lower Riser Transition (A023.202)	Pm	
	Pm+Pb	
	τ	
Lower Riser Spacer (A023.203)	Pm	
	Pm+Pb	
	τ	
ICIGT Support (A023.210)	N/A(1)	}}2(a),(c)

CRA Guide Tube Support Plate (A023.230)	Pm	{{
	Pm+Pb	
CRA Guide Tube (A023.231),CRDS Alignment Cone (A023.232),CRA Card (A023.233),CRA Lower Flange (A023.234)	Pm	
	Pm+Pb	
	σbearing	
CRA Guide Tube (A023.231)	Compressive stress, σbu_c	
	Combined axial compression and bending, NF-3322.1(e)(1), eq. 20, σbu_cs_20	
	Combined axial compression and bending, NF-3322.1(e)(1), eq. 21, σbu_cs_21	
	Combined axial compression and bending, NF-3322.1(e)(1), eq. 22, σbu_cs_22	
Fuel Pin and Cap (A023.250, A023.251, A023.061)	Pm+Pb	
	τ	
Core Barrel (A023.009)	Pm	
	Pm+Pb	
	τ	
	Compressive stress, σbu_c	
	Combined axial compression and bending, NF-3322.1(e)(1), eq. 20, σbu_cs_20	
	Combined axial compression and bending, NF-3322.1(e)(1), eq. 21, σbu_cs_21	
	Combined axial compression and bending, NF-3322.1(e)(1), eq. 22, σbu_cs_22	
Reflector Block (A023.044, A023.045, A023.046)	Pm	
	Pm+Pb	
	τ	
	σbearing	
Upper Support Block (A023.047)	Pm	
	Pm+Pb	
	σbearing	
	τ	
Reflector Block Alignment Pin (A023.049)	τ	
	σbearing	
Lower Core Plate (A023.008)	Pm	
	Pm+Pb	
	τ	
	σbearing	
Socket Head Cap Screw (A011.043)	Tensile stress in screw, σns	
	Shear stress in screw threads, τs	
	Shear stress in upper support block threads, τn	}}[2(a),(c)]

Control Rod Drive Shaft (All Parts of Assembly)	Pm	{{
	Pm+Pb	
Hex Head Cap Screw 1.25-12UN-4.5IN (A010.075)	Tensile stress in screw, σns	
	Shear stress in screw threads, τs	
	Shear stress in upper support block threads, τn	
Core Support Block Gusset (A011.040, A011.041)	Pm	
	Pm+Pb	
	τ	
Core Support Block Top Plate (A011.042)	Pm	
	Pm+Pb	
	τ	
	σbearing	
Alignment Dowel (A011.045)	τ	}}[2(a)(c)]

Note:

1. This component is similar in location and configuration to the lowest upper CRD shaft support. Thus, the evaluation of the CRD shaft support is used to determine acceptability of the ICIGT support.

Table A-11. Location of components where stress ratio is greater than 0.8

Item (Part Number)	Location
Upper CRDS Support (A023.305)	Bottom Upper CRDS Support
CRA Guide Tube Support Plate (A023.230)	In the support plate where the ring transitions to one of the four horizontal bars
Hex Head Cap Screw 1.25-12UN-4.5IN (A010.075)	Tensile stress in screw

Table A-12. ASME BPVC compliance - welds

Item 1 (Part Number)	Item 2 (Part Number)	Stress Type	Stress Ratio
Upper Riser Hanger Brace (A023.307)	Upper Riser Hanger Ring (A023.306)	Pm	{{
		Pm+Pb	
		T	
Upper Riser Hanger Brace (A023.307)	Upper Riser Section (A023.301)	Pm	
		Pm+Pb	
		T	
Upper CRDS Support (A023.305)	Upper Riser Section (A023.301)	Pm	
		Pm+Pb	
		T	
Upper Riser Bellows (A023.310)	Upper Riser Transition (A023.300)	Pm	
		Pm+Pb	
		T	
ICIGT Support (A023.210)	Lower Riser Transition (A023.202)	N/A(1)	
Lower Riser Spacer (A023.203)	Lower Riser Section (A023.201)	Pm	
		Pm+Pb	
		T	
Lower Riser Section (A023.201)	Upper Core Plate (A023.200)	Pm	
		Pm+Pb	
		T	
CRA GTSP (A023.230)	Lower Riser Spacer (A023.203)	Pm	
		Pm+Pb	
		T	
CRA Guide Tube (A023.231)	CRA Alignment Cone (A023.232)	T	
CRA Card (A023.233)	CRA Guide Tube (A023.231)	T	
CRA Lower Flange (A023.234)	CRA Guide Tube (A023.231)	T	
Upper Support Block(A023.048)	Core Barrel (A023.009)	Pm	
		Pm+Pb	
		T	
Core Barrel (A023.009)	Lower Core Plate (A023.008)	Pm	
		Pm+Pb	
		T	
Upper Riser Section (A023.301)	Upper Riser Bellows (A023.310)	N/A(2)	
Lower Riser Transition (A023.202)	Lower Riser Spacer (A023.203)	Pm	
		Pm+Pb	
		T	}}2(a)(c)

Notes:

1. The weld evaluation is bounded by the evaluation for the upper CRD shaft-upper riser section weld.
2. The weld evaluation is bounded by the evaluation for the upper riser bellows-upper riser transition weld.

Table A-13. Location of welds where stress ratio is greater than 0.8

Item 1 (Part Number)	Item 2 (Part Number)	Location
Upper Riser Hanger Brace (A023.307)	Upper Riser Hanger Ring (A023.306)	Corner of the brace top, where a brace is welded to the upper riser hanger ring

Table A-14. Maximum CRD shaft grid relative displacements (inch)

	ΔX (Hori.)	**ΔY (Vert.)**	**ΔZ (Hori.)**	**Horizontal Final**
Grid 1~2	{{			
Grid 2~3				
Grid 3~4				
Grid 4~5				}}2(a)(c)

{{

}}2(a)(c)

Figure A-1. Upper core plate model and boundary conditions

{{

}}2(a)(c)

Figure A-2. Lower core plate boundary conditions

{{

}}2(a)(c)

Figure A-3. Upper riser hanger ring boundary conditions

{{

}}2(a)(c)

Figure A-4. CRA model

{{

}}2(a)(c)

Figure A-5. Location of pilot nodes

{{

}}2(a)(c)

Figure A-6. CRA bonded connections

{{

}}2(a)(c)

Figure A-7. Control rod mass locations for three cases

{{

}}2(a)(c)

Figure A-8. CRA GTSP model

{{

}}2(a)(c)

Figure A-9. Upper riser assembly model

{{

}}2(a)(c)

Figure A-10. Bellows profile and constraint location

{{

}}2(a)(c)

Figure A-11. Constraints at URA

{{

}}2(a)(c)

Figure A-12. CRD shaft FE mesh

{{

}}2(a)(c)

Figure A-13. CRD shaft supports

{{

}}2(a)(c)

Figure A-14. Modal analysis results for CRA_1

{{

}}2(a)(c)

Figure A-15. First major mode shape for CRA_1

{{

}}2(a)(c)

Figure A-16. Modal analysis results for URA

{{

}}2(a)(c)

Figure A-17. First major lateral mode shape for URA

{{

}}2(a)(c)

Figure A-18. CRD shaft major modes and mode shapes

{{

}}2(a)(c)

Figure A-19. LCP stress intensity

{{

}}2(a)(c)

Figure A-20. Location of path lines for LCP

{{

}}2(a)(c)

Figure A-21. Upper riser hanger ring stress intensity

{{

}}2(a)(c)

Figure A-22. Location of path lines for upper riser hanger ring

{{

}}2(a)(c)

Figure A-23. CRA GTSP stress intensity and stress classification line locations

Attachment B

SG Assembly

General Information

Detailed stress analysis for the steam generator (SG) assembly under Service Level D conditions was performed in accordance with the American Society for Mechanical Engineers (ASME) Boiler and Pressure Vessel Code (BPVC). Analysis details and stress results are summarized below.

The components and welds included in the SG assembly evaluation are:

1. SG tubes
2. SG tube support column assemblies
3. Upper SG supports & associated welds
4. Lower SG supports & associated welds

In this evaluation, a 3D ANSYS model of the SG assembly, reactor pressure vessel (RPV), and the upper riser is used. A modal analysis is performed up to a minimum of 100 Hz to capture the dynamic effect due to seismic events and is followed by mode superposition multiple point response spectrum (MPRS) analysis to calculate the seismic response. The loss of coolant accident (LOCA) acceleration, dead weight, and pressure are analyzed using static analysis.

Input loading

The load combinations applicable to this analysis are provided in Table B-1. Each of the loads provided in Table B-1 is discussed below.

1. Pressure (P): Per the Design Specification, the maximum primary/secondary side pressure is {{ }}$^{2(a),(c)}$ psia. This maximum pressure is added to the maximum acoustic time history pressure of {{ }}$^{2(a),(c)}$ psia (determined from LOCA loading, below) such that a total Level D pressure applied is {{ }}$^{2(a),(c)}$ psia.

2. Deadweight (DW): The deadweight of the SG items, identified within the scope of this calculation, is captured by applying a linear acceleration of 386.089 in/s^2 in the positive vertical direction to simulate the downward effect of gravity.

3. Buoyancy (B): Buoyancy is not included and therefore the full DW is considered. This provides minimal conservatism as the full DW contributes a small amount of stress to the final stress as compared to other applicable Level D loads.

4. External mechanical loads (EXT): The only applicable EXT loads are the reaction forces at RPV-RVI interfaces. These are captured via model boundary conditions and connections (see Boundary conditions information under the Component structural modeling description).

5. Piping mechanical or thermal loads (M): There are no applicable M loads for the SG model.

6. Rod ejection accident (REA): REA is not applicable to the SG model.

7. MSLB/FWLB: Water hammer loads from a main steam line break (MSLB) or feedwater line break (FWLB) are compared to the maximum Level D acoustic pressure from a LOCA. The water hammer loads are smaller than the acoustic pressure load; therefore, MSLB and FWLB are not included in the analysis. The water hammer loads are developed using thermal hydraulic software.

   NRELAP5 is used to generate the fluid conditions within the steam generator for the MSLB and FWLB transients. The plot files created by NRELAP5 are post-processed with Python scripts that use a momentum balance to convert the fluid conditions in the NRELAP5 model to forces on the SG tubes. Steady-state forces are subtracted in order to give transient forces for comparison to the transient acoustic pressure LOCA forces. The maximum water hammer loads for FWLB and MSLB per unit length are {{ }}$^{2(a),(c)}$ and {{ }}$^{2(a),(c)}$, respectively. Figure B-1 and Figure B-2 are plots of the transient water hammer loads for the SG cells with the maximum load for the two transients.

   The maximum Level D acoustic pressure is {{ }}$^{2(a),(c)}$ psia. Using a control volume around the fluid in a section of SG tube with similar length to the NRELAP5 cell lengths, a force per unit length is calculated based on this acoustic pressure. The control volume sees a force equal to the pressure times the cross sectional area at each end of the section of tube. A net radial force is developed on the tube due to changing direction of the tube as it arcs. The total force acting on the tube due to the pressure is {{ }}$^{2(a),(c)}$ in the radial direction of the arc.

The maximum water hammer force is bounded by the maximum Level D acoustic pressure force: {{ }}[2(a),(c)] for the acoustic pressure compared to {{ }}[2(a),(c)] for water hammer. Water hammer forces due to MSLB and FWLB may thus be neglected in the load combinations for the Level D stress analysis.

8. SCRAM (SCR): SCRAM loads due to the drop of the CRD shaft and the control rod assembly (CRA) do not affect the SG stress analysis.

9. Safe-shutdown earthquake (SSE): SSE response spectra for the SG assembly are obtained at locations on the upper and lower risers and at the top and bottom of the SG for the MPRS analysis. Bounding spectra from locations on the upper riser and the lower riser transition are developed for the lower end of the upper riser. The broadened enveloped in-structure response spectra (ISRS) with 4% damping at the applicable locations are utilized to generate bounding spectra for application within this analysis. Figure B-3 through Figure B-5 present the seismic response spectra used in this evaluation.

10. LOCA (DBPB): In-structure LOCA response spectra with a 4% damping ratio are obtained at the same locations referenced for the SSE response spectra. The maximum spectrum accelerations are {{ }}2(a),(c) in the horizontal X direction, {{ }}[2(a),(c)] in the vertical direction, and {{ }}[2(a),(c)] in the horizontal Z direction. These values are applied statically in the LOCA evaluation portion with a factor of 1.5.

    LOCA acoustic pressures are obtained at locations in the riser and downcomer {{ }}[2(a),(c)], and near the upper riser at the pressurizer baffle plate {{ }}[2(a),(c)]. For these locations, a maximum acoustic pressure of {{ }}[2(a),(c)] psia is identified. This value was multiplied by a factor of 1.5 to obtain a maximum acoustic pressure of {{ }}[2(a),(c)] is used in this evaluation). This pressure was added to the Level D maximum pressure identified above and applied statically in the LOCA evaluation. Thus, the total Level D pressure applied is {{ }}[2(a),(c)] psia

This evaluation considers the following Service Level D load combination for the primary stress qualification:

|P+DW|+SRSS(SSE,LOCA)

where SRSS is the square root sum of the squares.

When considering the LOCA load combinations for the X, Y (vertical), and Z axes and the acoustic pressures (primary = {{ }}[2(a),(c)] psia and secondary = {{ }}[2(a),(c)] psia, denoted by Max+AccP1; primary = {{ }}[2(a),(c)] psia and secondary = {{ }}[2(a),(c)] psia, denoted by Max+AccP2), the load combinations in Table B-2 are evaluated within this calculation.

Component structural modeling

1. Overview

   A 3D ANSYS model was created wherein the SG tubes are modeled as BEAM189 elements. The element type was modified to PIPE288 in order to apply appropriate tube pressure. The model consists of 21 SG tube columns and 21 x 8 SG tube support assemblies. Tube columns 1, 11, and 21 are explicitly modeled while the other tube columns are represented by two super elements (ANSYS Matrix50 element): one super element for tube columns 2-10 and the other for columns 12-20. Super element use for the tube models is necessary due to the large number of degrees of freedom. The RPV and the upper riser are partially modeled to provide proper boundary conditions to the SG model. Due to the large number of degrees of freedom in the RPV and upper riser model, the RPV and upper riser model was converted to a super element, with the nodes interfacing with SG tube supports selected as master nodes. The SG top section edge, the SG bottom section edge, the lower end of the upper riser edge, the upper SG supports, and the lower SG supports are also selected as master nodes to apply boundary conditions and connections. The SG model and the adjacent upper riser and RPV are illustrated in Figure B-6. The number of elements in each super element are listed in Table B-3.

2. Fluid modeling and mass distribution

   a. Secondary water in SG tubes: Average densities of the liquid and steam secondary water are calculated for 11 regions over the height of the SG, with finer spatial discretization where the transition from liquid to steam occurs. The average densities are calculated based on thermal hydraulic model outputs and are used to develop effective densities for the tubes in the ANSYS model, accounting for both metal and water mass.

b. Primary coolant outside SG tubes: Primary coolant densities are calculated for the same 11 regions discussed above for the secondary water density calculation. The mass of fluid displaced by the SG tubes is applied to the tubes by including it in the effective tube densities.

c. Primary coolant surrounding tube supports: An effective density of the tube supports that includes the displaced fluid mass is applied in the ANSYS model.

d. Primary fluid hydrodynamic effect on RPV and riser: MASS21 elements are used to apply the mass of fluid contained inside the upper riser and upper RPV region near the baffle plate to the appropriate surfaces. Hydrodynamic coupling between the RPV and upper riser is accomplished using FLUID38 elements. Volume corrections are made in the fluid elements to subtract the tube and tube support volumes from the nominal annulus volume. Additionally, the FLUID38 element density is reduced to account for the fact that the displaced primary fluid mass is added to the densities of the tubes and tube supports in order to characterize the hydrodynamic effect for those components.

3. Tube support-to-tube support gap considerations

   At each support location, the tube support-to-tube support radial force is carried by the support tabs, not the tubes. A large force on the tab is required to close the diametric gaps and distribute load to the SG tubes. The force on the tab due to Level D loading is significantly lower than the force required to close the gaps. Thus, the radial force at the tube support is only distributed to the tabs, not to the tubes.

4. Boundary conditions

   The super element for the RPV and upper riser, the two super elements for SG tubes in Columns 2-10 and 12-20 (including both SG tubes and tube supports), and the three non-super-element tube columns (1, 11, and 21) are combined to form the final model using ANSYS parametric design language (APDL). The connections applied to the combined model are summarized in Table B-4.

5. Tube Support modeling
   Tube supports are modeled using BEAM188 elements with a rectangular section (see Figure B-7 for a view of the tube support beam model). The cross section width and height parameters are calculated to represent the equivalent bending stiffness in both

the strong and weak bending directions of a true configuration Solid model, shown in Figure B-14. This is done by first performing a static analysis on the Solid model, where the bottom surface is fixed and the top surface is applied with a unit force along the Z axis and X axis in two separate steps. The resultant directional displacements (δz and δx) at the top surface are then used in a generic beam deflection formula, $\delta = PL^3/3EI$, to solve for the two unknown cross section parameters for the Beam model.

Acceptance criteria

Per ASME BPVC, Section III, Paragraph NB-3225 and NG-3225, the rules in Section III Nonmandatory Appendix F may be used in evaluating Service Level D (Faulted Condition) loads. Therefore, Appendix F, Paragraph F-1331, “Criteria for Components” is used in the evaluation. Note that per Design Specification, the SG tubes shall be treated as a shell in accordance with Table NB-3217-1.

The material design stress intensity, S_m, the material yield strength, S_y, and the material ultimate strength, S_u, are taken from ASME BPVC, Section II, Part D at a temperature of 600°F.

The following qualification criteria are applicable:

1. F-1331.1 for general primary membrane stresses, local primary membrane stresses, general or local membrane plus bending primary stresses and average primary pure shear stress.
2. NB-3227 (SG tubes) and NG-3227 (SG supports) for special stress limits

Applicable Service Level D stress limits are summarized in Table B-5.

The upper and lower SG supports are welded to the RPV with a full penetration bevel weld. In accordance with the design specification, the welds between the upper and lower SG supports and the integral steam plenum and RPV shell are part of the RPV and constructed in accordance with ASME BPVC, Section III, Subsection NB, where no weld quality factors are required.

The SG tube and SG tube support deflections in the cylindrical coordinate systems are extracted for the load cases. The maximum deflections are found for radial, circumferential and vertical directions. There are no specific limits for the deflections. Deflections are provided for information only.

Results

1. Modal results

   The significant mode in each direction is listed in Table B-6, and plotted in Figure B-16 through Figure B-18. Note that the total simulated mass participation ratios are {{ }}[2(a),(c)] for X, Y and Z directions, respectively. The low total ratios are due to the fact that the RPV has the majority of the mass ({{ }}[2(a),(c)]) which is not activated with significant effective mass at lower frequencies.

2. Stress results

   The maximum membrane stress intensity (P_m), membrane plus bending stress intensity ($P_m + P_b$), and shear stress in the SG assembly components and associated welds are provided in Table B-7 through Table B-12. The locations of the stress results provided in Table B-7, Table B-8, Table B-11, and Table B-12 are indicated in Figure B-15. The bounding stress location for the SG tube (Column 21 listed in Table B-10) is indicated in Figure B-19. Note that the membrane stress for SG tube is calculated as the sum of axial stress and bending stress, because bending stress is classified as a membrane stress per ASME BPVC, Section III, Table NB-3217-1.

3. Deflections

   The deflections in the SG tubes and the SG tube supports are provided in Table B-13 and Table B-14, respectively.

Conclusions

The analysis described above demonstrates that the design of the SG assembly - specifically the SG tubes, the SG tube support assembly, the upper and lower SG supports, and the SG support welds - satisfies the structural requirements of the ASME BPVC for Service Level D loads.

Table B-1. Service Level D load combinations

Plant Event	Service Level	Load Combination	Allowable Limit
Rod Ejection Accident	D	P + DW + B + EXT + M + REA + SCR	Level C
Main Steam and Feedwater Pipe Breaks		P + DW + B + EXT + M + MSLB/FWLB+ SCR	Level D
SSE + DBPB/MSLB/FWLB		P + DW + B + EXT + M + SCR ± SRSS(1)(SSE + DBPB(2)/MSLB/FWLB)	Level D
Hydrogen Detonation with DDT		P + DW + B + EXT + HDDT	Level D

Note (1): SRSS is the square root sum of the squares
Note (2): DBPB loads are LOCA loads

Table B-2. Overall load steps

Load Step No.	Description
1	SRSS(SSE, LOCA (+X,+Y,+Z)) + P (Max+AccP1) + DW
2	SRSS(SSE, LOCA (+X,+Y,-Z)) + P (Max+AccP1) + DW
3	SRSS(SSE, LOCA (+X,-Y,+Z)) + P (Max+AccP1) + DW
4	SRSS(SSE, LOCA (+X,-Y,-Z)) + P (Max+AccP1) + DW
5	SRSS(SSE, LOCA (-X,+Y,+Z)) + P (Max+AccP1) + DW
6	SRSS(SSE, LOCA (-X,+Y,-Z)) + P (Max+AccP1) + DW
7	SRSS(SSE, LOCA (-X,-Y,+Z)) + P (Max+AccP1) + DW
8	SRSS(SSE, LOCA (-X,-Y,-Z)) + P (Max+AccP1) + DW
9	SRSS(SSE, LOCA (+X,+Y,+Z)) + P (Max+AccP2) + DW
10	SRSS(SSE, LOCA (+X,+Y,-Z)) + P (Max+AccP2) + DW
11	SRSS(SSE, LOCA (+X,-Y,+Z)) + P (Max+AccP2) + DW
12	SRSS(SSE, LOCA (+X,-Y,-Z)) + P (Max+AccP2) + DW
13	SRSS(SSE, LOCA (-X,+Y,+Z)) + P (Max+AccP2) + DW
14	SRSS(SSE, LOCA (-X,+Y,-Z)) + P (Max+AccP2) + DW
15	SRSS(SSE, LOCA (-X,-Y,+Z)) + P (Max+AccP2) + DW
16	SRSS(SSE, LOCA (-X,-Y,-Z)) + P (Max+AccP2) + DW

Note: The pressure combinations include a one (1) g acceleration to account for deadweight of the configuration.

Table B-3. Number of elements in each super element

Component	Number of elements
RPV and upper riser	16,582
Columns 2 through 10	113,332
Columns 12 through 20	125,448

Table B-4. Summary of component connections (1: coupled, 0: uncoupled)

Component	UX	UY	UZ	ROTX	ROTY	ROTZ	Coord. System
SG tube - Tube support tab (Figure B-7)	1	1	1	0	1	1	local
Tube support top - Upper SG support (Figure B-8)	1	1	1	1	0	1	Global cylindrical
Tube support bottom - Lower SG support (Figure B-9)	0	1	0	0	0	0	Global cylindrical
Tube support tab tip - Tube support back (Figure B-10)	1	1	0	0	0	1	Global cylindrical
RPV shell - Col. 21 tube support back (Figure B-11)	1	1	0	0	0	1	Global cylindrical
Col. 1 tube support tab tip - RVI shell (Figure B-12)	1	1	0	0	0	1	Global cylindrical
SG tube - Tubesheet (Figure B-13)	1	1	1	1	1	1	Global Cartesian

Table B-5. Allowable stress limits for Service Level D

ASME Stress Category	ASME Code Paragraph	ASME Criterion
General Primary Membrane Stress Intensity, P_m	F-1331.1(a)	lesser of $2.4S_m$ and $0.7S_u$
Local Primary Membrane Stress Intensity,P_l	F-1331.1(b)	1.5 P_m
General or Local Primary Membrane plus Bending Stress Intensity for components other than SG tubes, P_m+P_b	F-1331.1(c)(1)	1.5 P_m
Compressive Loads (SG Tubes) Allowable External Pressure	F-1331.5(b), Note 1	1.5 x (P_a)
Average Primary Pure Shear Stress	SG Tubes NB-3225, F-1331.1(d) SG Supports NG-3225, NG-3227, NG-3227.2	SG Tubes $0.42S_u$ SG Supports $1.2S_m$

Note:

1. Allowable external pressure (P_a) as calculated by NB-3133 is greater than or equal to the external pressure (P). Alternatively, the rules of ASME Code Case N-759-2 may be used.

Table B-6. Significant modes

Direction	Freq. (Hz)	Effective Mass (Slug)	Ratio	Total simulated participation ratio
X	{{			
Y				
Z				}}[2(a),(c)]

Table B-7. Bounding stresses in upper portion of SG tube supports

	Max Stress (psi)	Allowable Stress (psi)	Load Step	Stress Ratio	Passed
P_m	{{				Yes
P_m+P_b					Yes
Shear				}}[2(a),(c)]	Yes

Table B-8. Bounding stresses in lower portion of SG tube supports

	Max Stress (psi)	Allowable Stress (psi)	Load Step	Stress Ratio	Passed
P_m	{{				Yes
P_m+P_b					Yes
Shear				}}[2(a),(c)]	Yes

Table B-9. Bounding stresses in SG tube support tabs

(a) Tabs providing radial supports

	Max Stress (psi)	Allowable Stress (psi)	Load Step	Stress Ratio	Passed
P_m	{{				Yes
P_m+P_b					Yes
Shear				}}[2(a),(c)]	Yes

(b) Tabs providing circumferential supports

	Max Stress (psi)	Allowable Stress (psi)	Load Step	Stress Ratio	Passed
P_m	{{				Yes
P_m+P_b					Yes
Shear				}}[2(a),(c)]	Yes

Table B-10 Bounding stresses in SG tubes

		Max Stress (psi)	Allowable Stress (psi)	Load Step	Stress Ratio	Passed
Col. 1	P_m	{{				Yes
	Shear					Yes
Col. 11	P_m					Yes
	Shear					Yes
Col. 21	P_m					Yes
	Shear				}}[2(a),(c)]	Yes

Table B-11. Bounding stresses in the upper SG support welds

Circ.Location		Max Stress (psi)	Allowable Stress (psi)	Stress Ratio	Passed
1	P_m	{{			Yes
	P_m+P_b				Yes
	Shear				Yes
2	P_m				Yes
	P_m+P_b				Yes
	Shear				Yes
3	P_m				Yes
	P_m+P_b				Yes
	Shear				Yes
4	P_m				Yes
	P_m+P_b				Yes
	Shear				Yes
5	P_m				Yes
	P_m+P_b				Yes
	Shear				Yes
6	P_m				Yes
	P_m+P_b				Yes
	Shear				Yes
7	P_m				Yes
	P_m+P_b				Yes
	Shear				Yes
8	P_m				Yes
	P_m+P_b				Yes
	Shear			}}[2(a),(c)]	Yes

Table B-12. Bounding stresses in the lower SG support welds

Circ.Location		Max Stress (psi)	Allowable Stress (psi)	Stress Ratio	Passed
1	P_m	{{			Yes
	P_m+P_b				Yes
	Shear				Yes
2	P_m				Yes
	P_m+P_b				Yes
	Shear				Yes
3	P_m				Yes
	P_m+P_b				Yes
	Shear				Yes
4	P_m				Yes
	P_m+P_b				Yes
	Shear				Yes
5	P_m				Yes
	P_m+P_b				Yes
	Shear				Yes
6	P_m				Yes
	P_m+P_b				Yes
	Shear				Yes
7	P_m				Yes
	P_m+P_b				Yes
	Shear				Yes
8	P_m				Yes
	P_m+P_b				Yes
	Shear			}}[2(a),(c)]	Yes

Table B-13. Maximum deflection in SG tubes

	Deflection (in)		
Column	**Radial**	**Hoop**	**Vertical**
1	{{		
11			
21			}}[2(a),(c)]

Table B-14. Maximum deflection in SG tube supports

	Deflection (in)		
Column	**Radial**	**Hoop**	**Vertical**
1	{{		
11			
21			}}[2(a),(c)]

{{

}}2(a),(c)

Figure B-1. Transient force on SG cell with maximum FWLB load

{{

}}2(a),(c)

Figure B-2. Transient force on SG cell with maximum MSLB load

{{

}}[2(a),(c)]

Figure B-3. Bounding seismic spectra in X

{{

}}[2(a),(c)]

Figure B-4. Bounding seismic spectra in Y

{{

}}2(a),(c)

Figure B-5. Bounding seismic spectra in Z

{{

}}2(a),(c)

Figure B-6. SG model and the adjacent upper riser and RPV

{{

}}2(a),(c)

Figure B-7. SG tube - tube support tab connections (column 21 shown)

{{

}}2(a),(c)

Figure B-8. Tube support top - upper SG support connections. Shown on non-super-element model. For visualization purposes only.

{{

}}2(a),(c)

Figure B-9. Tube support bottom - lower SG support connections. Shown on non-super-element model. For visualization purposes only.

{{

}}2(a),(c)

Figure B-10. Tube support tab tip - tube support back connections. Shown for column 12 through 20 submodel before super element reduction.

{{

}}2(a),(c)

Figure B-11. RPV shell - Col. 21 tube support back connections. RPV shown explicitly (non-super-element) for visualization purposes only.

{{

}}[2(a),(c)]

Figure B-12. Col. 1 tube support tab tip - RVI shell connections. RVI shown explicitly (non-super-element) for visualization purposes only.

{{

}}2(a),(c)

Figure B-13. SG tube - tubesheet connections. Shown on non-super-element model. For visualization purposes only.

{{

}}2(a),(c)

Figure B-14. Detailed tube support model mesh

{{

}}2(a),(c)

Figure B-15. Tube support and SG support base metal and weld stress locations

{{

}}2(a),(c)

Figure B-16. Significant mode in X

{{

}}2(a),(c)

Figure B-17. Significant mode in Y

{{

}}2(a),(c)

Figure B-18. Significant mode in Z

{{

}}2(a),(c)

Figure B-19. Bounding stress location in SG tubes

Attachment C - CRDS and CRAGT Gap Evaluation

Question RVI 1 (original text) - ASME Section III Appendix F-1321.3 requires consideration of gaps between part of the structures. CRDS and CRAGT have diametric gap as below.

	CRDS	CRAGT
Diametric Gap (in)	{{	}}$^{2(a),(c)}$

Data from {{

}}$^{2(a),(c)}$

Describe the boundary conditions at the diametric gaps (fixed or free) of CRDS and CRAGT and provide justification for not considering the gaps.

NuScale response - The boundary conditions and justification for not considering the gaps for the control rod assembly guide tube (CRAGT) and control rod drive system (CRDS) are described separately below.

CRAGT

The CRAGT is one of the four components included in the control rod assembly (CRA) model, as shown in Figure C-1. In the CRA analysis, the bottom pilot node is fixed in all 6 degrees of freedom (DOFs), because the CRA Lower Flange is bolted to the Upper Core Plate. The top pilot node is also fixed in 6 DOFs. Although there is a {{ }}$^{2(a),(c)}$ inch radial gap between the CRDS Alignment Cone and the CRA Guide Tube Support Plate (see Figure C-2), the contact impact force is insignificant locally, because the gap size is small. Given that the sections in the nearby CRDS Alignment Cone and CRA Guide Tube Support Plate are large, the stress due to the contact impact force is negligible. Therefore, the gap was not modeled in the analysis.

CRDS

For the control rod drive (CRD) shafts in the upper riser assembly (URA) analysis, the tops are constrained in 6 DOFs and the steam plenum elevations are constrained in 4 DOFs (no vertical translational or torsional DOFs). Figure C-3 shows one of the 16 CRD shafts taken from the upper riser assembly (URA) analysis. The boundary conditions for the 16 CRD shafts are identical. The CRD shafts are also coupled to the CRDS supports (the five grids) in the horizontal translational DOFs.

To investigate the gap effects, an additional analysis was performed. This analysis used two models (one linear and the other nonlinear) similar to the CRD shaft-CRDS support components in the URA analysis. The linear model (L) and the nonlinear model (NL) only include one CRD shaft and related supports. The L model is similar to the model in Figure C-3 by coupling lateral translational DOFs. The NL model includes contact pairs at the radial gaps. Transient analyses are performed on these two models, and then their reaction forces, moments, and stresses at limiting locations are compared. If the stresses from the NL model are bounded by those from the L model, using the linear model in the URA analysis is acceptable.

The only difference between the L and NL models is whether the shaft is coupled to the supports. Both models are assigned “Standard” contact in ANSYS, but the L model is additionally assigned CP commands to couple lateral translational DOFs (Ux and Uz) of the shaft to the supports. A diagram of the model used in this evaluation is shown in Figure C-4. This diagram shows the element connectivity between keypoints. It also lists the section number for each line, which correlates to a given cross-section geometry for the beam elements. Real constants for each line are listed which indicate the contact-target element pairing between the CRD shaft and the supports. The CRDS supports 1 through 5 are defined as locations 4 through 8 in the FEM, to be consistent with the naming system used in the URA analysis. Locations 1 through 3 are the RPV head, steam plenum, and hanger ring, respectively.

The CRD shaft, guides and supports are meshed with 2-node BEAM188 elements, using the quadratic shape function. The maximum element length is set to 1.75 inch. CONTA176 elements are overlaid on the CRD shaft elements that pair with TARGE170 elements on the guides and supports. The contact-target pairs are indicated in Figure C-4. Due to the slenderness of the model, a single view of the model mesh does not show sufficient detail. Instead, different sections of the mesh are shown in Figure C-5.

Stainless steel material properties are assigned to the model with mass correction to account for the simplification of the model. Global Rayleigh damping is used in the transient analysis. The alpha and beta damping multipliers are calculated based on {{ }}[2(a),(c)] system damping ratio in the frequency range of {{ }}[2(a),(c)] Hz. This frequency range, determined from modal analysis, covers the major modes of the shaft.

All 12 seismic time-history cases from the NPM Seismic Analysis technical report TR-0916-51502 Section 8.0 are evaluated. Displacement time histories are applied to the top of the shaft and supports. The keypoints 715, 716, and 208 are above the RPV head in the NPM and therefore are applied with the same displacements as those used on the Shaft top (location 1) in Figure C-3. The integral steam plenum (keypoint 714) and upper riser hanger ring (keypoint 713) are connected, so they are both applied with the same displacements as those used on the

location 2 in Figure C-3. The five CRDS supports are applied with displacements as those used on locations 4 through 8, respectively.

Reaction forces and moments are extracted at eight bounding locations. These locations are illustrated in Figure C-6. In addition, the Pm and Pm+Pb stresses are calculated at these locations. Displacement data at supports and corresponding shaft locations, as well as their contact status are also extracted. The resultant displacement data showed that the maximum relative displacement between supports and corresponding shaft locations in the NL model is about {{ }}[2(a),(c)] inch, demonstrating that the contact elements work correctly.

An example of reaction force comparison (at location 1b for the RXM6_UC_StiffK case) from the two models is shown in Figure C-7. The moment comparison is shown in Figure C-8. Note that the “My” is not shown in Figure C-8 because there is no torsional moment on the shaft. The stress comparison is shown in Figure C-9. The minimum (negative value) and maximum (positive value) reactions summarized from all eight locations are listed in Table C-1 and Table C-2 for the NL and L models, respectively. The corresponding locations are also listed in these two tables.

From Figure C-7, the reaction forces are generally higher in the NL model. The impact force due to the contact causes higher reaction forces in the NL model. From Figure C-8, moment magnitudes are comparable in the two models. Figure C-9 shows that the highest stresses are also comparable in the two models. This is because the peak moment loads are the main contributors to stresses in the shafts, and thus the higher peak reaction forces in the NL model do not significantly affect resultant stresses.

By comparing the global max values of Pm and Pm+Pb in Table C-1 to those in Table C-2, it is observed that the stresses are higher in the L model than in the NL model. In location 2, the maximum reaction forces and moments are much higher in the L model than in the NL model (see Figure C-10 and Figure C-11). This is because in the L model the vibration near the location 2 at peak load time points are close to the first major mode, and thus the resonance causes large reactions. For example, Figure C-12 shows the time near the peak Fx in Figure C-10. It is found that a cycle of the response is from {{ }}[2(a),(c)] seconds, as shown in Figure C-12. This corresponds to a frequency of {{ }}[2(a),(c)], which is very close to the first major frequency {{ }}[2(a),(c)] Hz. On the other hand, the NL model vibrates at a higher frequency compared to the L model, and therefore the NL model reactions are lower. This is due to the nonlinear contact in the NL model changing the major frequencies of the shaft to be away from the transient load frequencies, so that resonance does not occur. Although there are impact forces between the contact surfaces, the impact forces are not significant because the gap size is small.

The minimum force and moment values for all twelve seismic time history cases are summarized in Table C-3, and the maximum force, moment, and stress values are summarized in Table C-4. There are some instances where the magnitude of the force and/or moment for an NL cases exceeds that of the corresponding L case; however, in all cases the stress values of the NL cases are below those of the corresponding L cases.

In conclusion, because the stresses from the nonlinear model are bounded by those from the linear model, using the linear model in the URA analysis (not considering the gap) is acceptable.

Table C-1. NL results for the representative “RXM6 UC StifK” seismic inputs

(a) Minimum value

Location	Fx (lbf)	Fy (lbf)	Fz (lbf)	Mx (in-lbf)	My (in-lbf)	Mz (in-lbf)
Loc1b	{{					
LocMid12						
Loc2						
Loc4b						
Loc5b						
Loc6b						
Loc7b						
Loc8b						}}2(a),(c)

Global min value	{{					
Global min location						}}2(a),(c)

(b) Maximum value

Location	Fx (lbf)	Fy (lbf)	Fz (lbf)	Mx (in-lbf)	My (in-lbf)	Mz (in-lbf)	Pm (psi)	PmPb (psi)
Loc1b	{{							
LocMid12								
Loc2								
Loc4b								
Loc5b								
Loc6b								
Loc7b								
Loc8b								}}2(a),(c)

Global max value	{{							
Global max location								}}2(a),(c)

Table C-2. L results for the representative “RXM6 UC StifK” seismic inputs

(a) Minimum value

Location	Fx (lbf)	Fy (lbf)	Fz (lbf)	Mx (in-lbf)	My (in-lbf)	Mz (in-lbf)
Loc1b	{{					
LocMid12						
Loc2						
Loc4b						
Loc5b						
Loc6b						
Loc7b						
Loc8b						}}2(a),(c)

Global min value	{{					
Global min location						}}2(a),(c)

(b) Maximum value

Location	Fx (lbf)	Fy (lbf)	Fz (lbf)	Mx (in-lbf)	My (in-lbf)	Mz (in-lbf)	Pm (psi)	PmPb (psi)
Loc1b	{{							
LocMid12								
Loc2								
Loc4b								
Loc5b								
Loc6b								
Loc7b								
Loc8b								}}2(a),(c)

Global max value	{{							
Global max location								}}2(a),(c)

Table C-3. Summary of minimum force and moment results from all seismic cases

Seismic case and boundary conditions	Fx (lbf)	Fy (lbf)	Fz (lbf)	Mx (in-lbf)	My (in-lbf)	Mz (in-lbf)
RXM1_CR_SoftK__L	{{					
RXM1_CR_SoftK_NL						
RXM1_CR_NomiK__L						
RXM1_CR_NomiK_NL						
RXM1_CR_StifK__L						
RXM1_CR_StifK_NL						
RXM1_UC_SoftK__L						
RXM1_UC_SoftK_NL						
RXM1_UC_NomiK__L						
RXM1_UC_NomiK_NL						
RXM1_UC_StifK__L						
RXM1_UC_StifK_NL						
RXM6_CR_SoftK__L						
RXM6_CR_SoftK_NL						
RXM6_CR_NomiK__L						
RXM6_CR_NomiK_NL						
RXM6_CR_StifK__L						
RXM6_CR_StifK_NL						
RXM6_UC_SoftK__L						
RXM6_UC_SoftK_NL						
RXM6_UC_NomiK__L						
RXM6_UC_NomiK_NL						
RXM6_UC_StifK__L						
RXM6_UC_StifK_NL						}}[2(a),(c)]

Table C-4. Summary of maximum force, moment, and stress results from all seismic cases

Seismic case and boundary conditions	Fx (lbf)	Fy (lbf)	Fz (lbf)	Mx (in-lbf)	My (in-lbf)	Mz (in-lbf)	Pm (psi)	Pm+Pb (psi)
RXM1_CR_SoftK__L	{{							
RXM1_CR_SoftK_NL								
RXM1_CR_NomiK__L								
RXM1_CR_NomiK_NL								
RXM1_CR_StifK__L								
RXM1_CR_StifK_NL								
RXM1_UC_SoftK__L								
RXM1_UC_SoftK_NL								
RXM1_UC_NomiK__L								
RXM1_UC_NomiK_NL								
RXM1_UC_StifK__L								
RXM1_UC_StifK_NL								
RXM6_CR_SoftK__L								
RXM6_CR_SoftK_NL								
RXM6_CR_NomiK__L								
RXM6_CR_NomiK_NL								
RXM6_CR_StifK__L								
RXM6_CR_StifK_NL								
RXM6_UC_SoftK__L								
RXM6_UC_SoftK_NL								
RXM6_UC_NomiK__L								
RXM6_UC_NomiK_NL								
RXM6_UC_StifK__L								
RXM6_UC_StifK_NL								}}2(a),(c)

{{

}}2(a)(c)

Figure C-1. CRA model components and boundary conditions

{{

}}2(a)(c)

Figure C-2. Gap between the CRDS Alignment Cone and CRA Guide Tube Support Plate

{{

}}2(a)(c)

Figure C-3. CRD Shaft boundary conditions in the URA analysis

{{

}}2(a)(c)

Figure C-4. Diagram of the CRD shaft model (elements are collinear, but are shown offset for clarity; not to scale)

{{

}}2(a)(c)

Figure C-5. Mesh of sections of the L and NL models

{{

}}2(a)(c)

Figure C-6. Post-processing locations

{{

}}2(a)(c)

Figure C-7. Reaction forces at location 1b for the NPM6_UC_StiffK case

{{

}}2(a)(c)

Figure C-8. Reaction moments at location 1b for the NPM6_UC_StiffK case

{{

}}2(a)(c)

Figure C-9. Resultant stresses at location 1b for the NPM6_UC_StiffK case

{{

}}2(a)(c)

Figure C-10. Reaction forces at location 2 for the NPM6_UC_StiffK case

{{

}}2(a)(c)

Figure C-11. Reaction moments at location 2 for the NPM6_UC_StiffK case

{{

}}2(a)(c)

Figure C-12. Resultant Fx at location 2 near highest peaks for the NPM6_UC_StiffK case

Impact on DCA:

There are no impacts to the DCA as a result of this response.

Enclosure 3:

Affidavit of Thomas A. Bergman, AF-0819-66531

NuScale Power, LLC
1100 NE Circle Blvd., Suite 200 Corvalis, Oregon 97330, Office: 541.360.0500, Fax: 541.207.3928
www.nuscalepower.com

NuScale Power, LLC

AFFIDAVIT of Thomas A. Bergman

I, Thomas A. Bergman, state as follows:

1. I am the Vice President, Regulatory Affairs of NuScale Power, LLC (NuScale), and as such, I have been specifically delegated the function of reviewing the information described in this Affidavit that NuScale seeks to have withheld from public disclosure, and am authorized to apply for its withholding on behalf of NuScale.
2. I am knowledgeable of the criteria and procedures used by NuScale in designating information as a trade secret, privileged, or as confidential commercial or financial information. This request to withhold information from public disclosure is driven by one or more of the following:
    a. The information requested to be withheld reveals distinguishing aspects of a process (or component, structure, tool, method, etc.) whose use by NuScale competitors, without a license from NuScale, would constitute a competitive economic disadvantage to NuScale.
    b. The information requested to be withheld consists of supporting data, including test data, relative to a process (or component, structure, tool, method, etc.), and the application of the data secures a competitive economic advantage, as described more fully in paragraph 3 of this Affidavit.
    c. Use by a competitor of the information requested to be withheld would reduce the competitor's expenditure of resources, or improve its competitive position, in the design, manufacture, shipment, installation, assurance of quality, or licensing of a similar product.
    d. The information requested to be withheld reveals cost or price information, production capabilities, budget levels, or commercial strategies of NuScale.
    e. The information requested to be withheld consists of patentable ideas.
3. Public disclosure of the information sought to be withheld is likely to cause substantial harm to NuScale's competitive position and foreclose or reduce the availability of profit-making opportunities. The accompanying Request for Additional Information response reveals distinguishing aspects about the method by which NuScale develops its power module seismic analysis.

    NuScale has performed significant research and evaluation to develop a basis for this method and has invested significant resources, including the expenditure of a considerable sum of money.

    The precise financial value of the information is difficult to quantify, but it is a key element of the design basis for a NuScale plant and, therefore, has substantial value to NuScale.

    If the information were disclosed to the public, NuScale's competitors would have access to the information without purchasing the right to use it or having been required to undertake a similar expenditure of resources. Such disclosure would constitute a misappropriation of NuScale's intellectual property, and would deprive NuScale of the opportunity to exercise its competitive advantage to seek an adequate return on its investment.

4. The information sought to be withheld is in the enclosed response to NRC Request for Additional Information No. 202, eRAI No. 8911. The enclosure contains the designation "Proprietary" at the top of each page containing proprietary information. The information considered by NuScale to be proprietary is identified within double braces, "{{ }}" in the document.
5. The basis for proposing that the information be withheld is that NuScale treats the information as a trade secret, privileged, or as confidential commercial or financial information. NuScale relies upon the exemption from disclosure set forth in the Freedom of Information Act ("FOIA"), 5 USC § 552(b)(4), as well as exemptions applicable to the NRC under 10 CFR §§ 2.390(a)(4) and 9.17(a)(4).
6. Pursuant to the provisions set forth in 10 CFR § 2.390(b)(4), the following is provided for consideration by the Commission in determining whether the information sought to be withheld from public disclosure should be withheld:
    a. The information sought to be withheld is owned and has been held in confidence by NuScale.
    b. The information is of a sort customarily held in confidence by NuScale and, to the best of my knowledge and belief, consistently has been held in confidence by NuScale. The procedure for approval of external release of such information typically requires review by the staff manager, project manager, chief technology officer or other equivalent authority, or the manager of the cognizant marketing function (or his delegate), for technical content, competitive effect, and determination of the accuracy of the proprietary designation. Disclosures outside NuScale are limited to regulatory bodies, customers and potential customers and their agents, suppliers, licensees, and others with a legitimate need for the information, and then only in accordance with appropriate regulatory provisions or contractual agreements to maintain confidentiality.
    c. The information is being transmitted to and received by the NRC in confidence.
    d. No public disclosure of the information has been made, and it is not available in public sources. All disclosures to third parties, including any required transmittals to NRC, have been made, or must be made, pursuant to regulatory provisions or contractual agreements that provide for maintenance of the information in confidence.
    e. Public disclosure of the information is likely to cause substantial harm to the competitive position of NuScale, taking into account the value of the information to NuScale, the amount of effort and money expended by NuScale in developing the information, and the difficulty others would have in acquiring or duplicating the information. The information sought to be withheld is part of NuScale's technology that provides NuScale with a competitive advantage over other firms in the industry. NuScale has invested significant human and financial capital in developing this technology and NuScale believes it would be difficult for others to duplicate the technology without access to the information sought to be withheld.

I declare under penalty of perjury that the foregoing is true and correct. Executed on August 2, 2019.

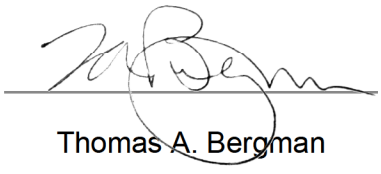

Thomas A. Bergman